

Model sensitivity of ice flux over the grounding line to present-day climatic forcing and geothermal flux

Session CR5.1: EGU2016-13747 X4.13



ALFRED-WEGENER-INSTITUT
HELMHOLTZ-ZENTRUM FÜR POLAR-
UND MEERESFORSCHUNG

T. Kleiner (thomas.kleiner@awi.de) and A. Humbert

Introduction

Large uncertainties remain in the current and future contribution to sea level change from Antarctica from observations and numerical flow modelling. Within the SeaRISE project (Bindschadler et al., 2013) atmospheric, oceanic, and subglacial forcing scenarios were applied to different ice-sheet models to assess Antarctic ice sheet sensitivity over a 500 year timescale. It has been shown, that the model results highly depend on the chosen climate forcing and spin-up strategy.

We use the Parallel Ice Sheet Model (PISM, Bueler and Brown, 2009) to perform spin-up simulations across different data sets providing present-day boundary conditions for the Antarctic Ice Sheet (surface temperature, surface mass balance and geothermal flux). The utilized spin-up methods include free evolving and geometry constrained simulations. Here we present our analysis of the ice flux over the grounding line for each set-up and compare the fluxes from large drainage basin units with estimates derived from remote sensing.

Model set-up

The Bedmap2 (Fretwell et al., 2013) datasets for ice thickness and bedrock elevation updated with data from the airborne radio-echo sounding campaign of the Alfred Wegener Institute in the Recovery Glacier drainage area (Jan. 2014) serve as the initial geometry for all simulations.

We have applied varying datasets for boundary conditions as: surface temperature (Comiso (2000), Fortuin and Oerlemans (1990) and Van Wessem et al. (2014)), surface mass balance (Arthern et al. (2006), Van de Berg et al. (2006) and Van Wessem et al. (2014)) and geothermal flux (Shapiro and Ritzwoller (2004), Fox Maule et al. (2005) and the update from Purucker (2012)). The original data set of Fox Maule et al. (2005) has been capped at a value of 0.07 W/m² according to the recommendation for the SeaRISE-Antarctica set-up (Bindschadler et al., 2013).

A present-day state of the Antarctic Ice Sheet has been computed for each combination of boundary conditions, with the restriction that RACMO2.3/ANT (Van Wessem and others, 2014) data for surface skin temperature and accumulation rate are used together for consistency. Thus an model ensemble based on 5 different surface forcings and 3 different heat fluxes is used. We further distinguish between simulations with a fixed geometry (FT, using PISM's Flux correction method for ice Thickness) and a free evolving geometry (SR1, cf. Potsdam model in SeaRISE-Antarctica, Nowicki et al., 2013). The SR2 simulations are similar to SR1, but with subgrid grounding line treatment (subgl, Feldmann et al., 2014).

Model spin-up

We mainly follow the spin-up strategy given in the searise-antarctica example that comes with PISM. After initial smoothing (100 a, non-sliding SIA) and 200 ka thermal spin-up with fixed geometry on a coarse grid (40 km), the present-day state of the Antarctic Ice Sheet has been computed in a series of subsequent grid refinements (all based on the initial 1km present day geometry) using 40 km (run length: 100 ka), 20 km (run length: 20 ka) and 10 km (run length: 4 ka) horizontal resolution and 41, 81 and 101 vertical layers, respectively.

Arthern et al. (2006). Antarctic snow accumulation mapped using polarization of 4.3-cm wavelength microwave emission. *Journal of Geophysical Research*, 111:D06107.
Bindschadler et al. (2013). Ice-sheet model sensitivities to environmental forcing and their use in projecting future sea level (the SeaRISE project). *Journal of Glaciology*, 59:195-224.
Bueler and Brown (2009). Shallow shelf approximation as a "sliding law" in a thermomechanically coupled ice sheet model. *Journal of Geophysical Research*, 114(F3): F03008.
Comiso (2000). Variability and trends in Antarctic surface temperatures from in situ and satellite infrared measurements. *Journal of Climate*, 13(10):1674-1696.
Feldmann et al. (2014). Resolution-dependent performance of grounding line motion in a shallow model compared to a full-Stokes model according to the MISIP3d intercomparison. *Journal of Glaciology*, 60: 353-360.
Fortuin and Oerlemans (1990). The parameterization of the annual surface temperature and mass balance of Antarctica. *Annals of Glaciology*, 14:78-84.
Fox Maule et al. (2005). Heat flux anomalies in Antarctica revealed by satellite magnetic data. *Science*, 309(5733):464-467.
Fretwell et al. (2014). Bedmap2: improved ice bed, surface and thickness datasets for Antarctica. *The Cryosphere*, 7(1):375-393.
Nowicki et al. (2013). Insights into spatial sensitivities of ice mass response to environmental change from the SeaRISE ice sheet modeling project I: Antarctica. *Journal of Geophysical Research: Earth Surface*, 118:1002-1024.

Model output processing

For each model output:

- Solve floating condition equation $\tau_{hk} + \rho_{osw}/\rho_{oi} \times \tau_{opg} = 0$ to get ordered points along the grounding line (GL) contour.
- Select longest contour as the main GL.
- Extract \bar{u} , \bar{v} , τ_{hk} from model output along the GL contour using bi-linear interpolation.
- Calculate outward pointing normal vector along the GL contour.
- Calculate local ice flux in the direction normal to the GL contour.
- Trace each point along the GL contour back to its drainage basin definition using 4th-order Runge-Kutta integrator based on the modelled flow field and assign the drainage basin number.
- Numerically integrate the flux along the GL contour using trapezoidal rule.

Results

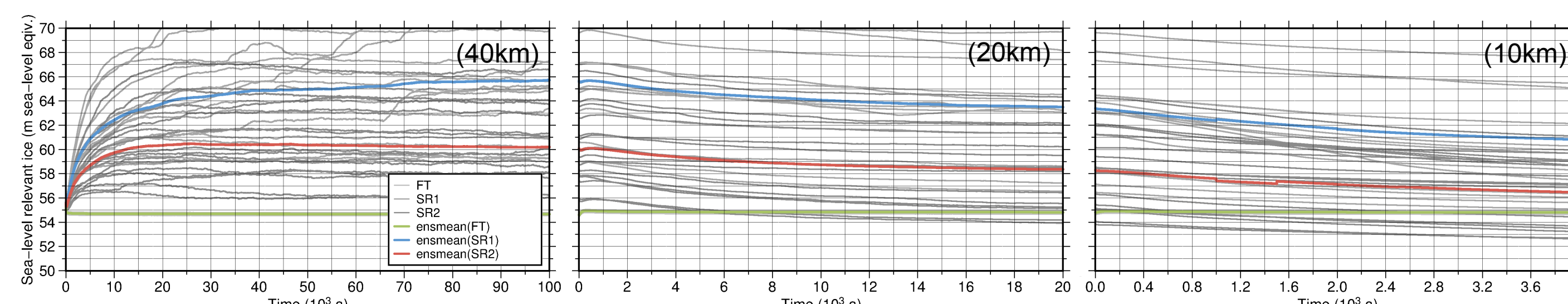


Fig. 1: Time series of modelled total sea-level equivalent ice volume (volume above flotation, VAF) in sea-level equivalent during the grid refinement steps (40km, 20km and 10km) for all simulations. The ensemble means for the fixed and free evolving geometry simulations FT, SR1 and SR2 are shown in green, blue and red respectively.

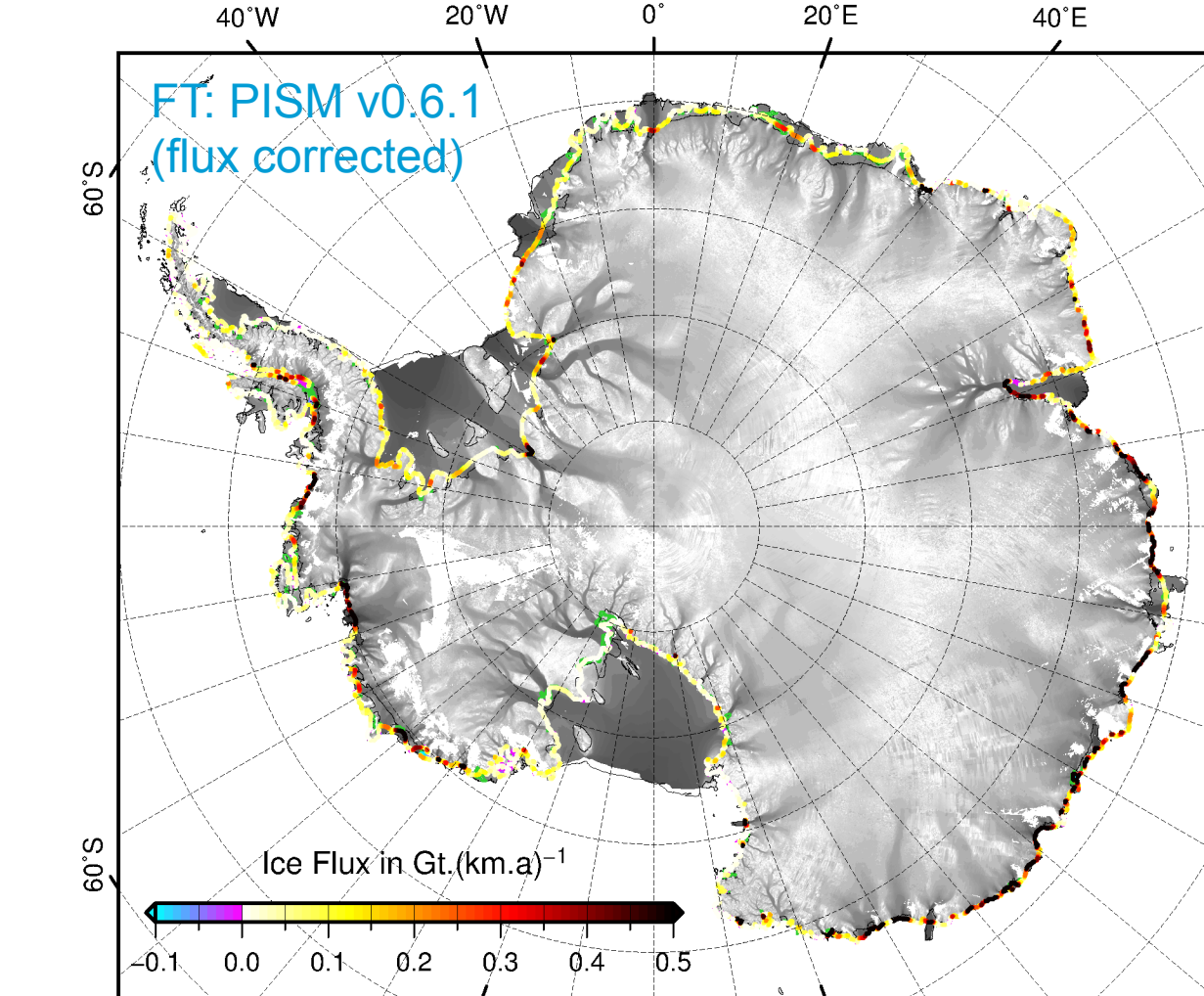


Fig. 2: Ensemble mean ice fluxes over the grounding line (GL) based on the ensemble simulations with various climatic boundary conditions all describing the present-day for the three spin-up types FT, SR1 and SR2. Green lines represent alternative GL positions within each ensemble. The observed present-day surface velocity (Rignot et al., 2008) is shown in grey in the background.

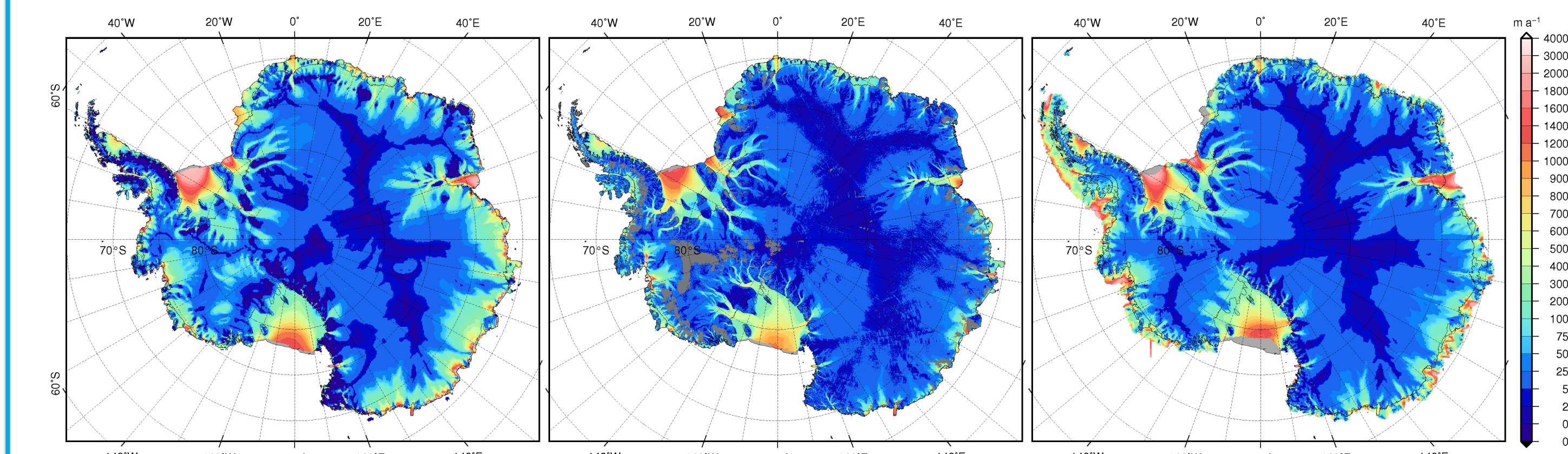
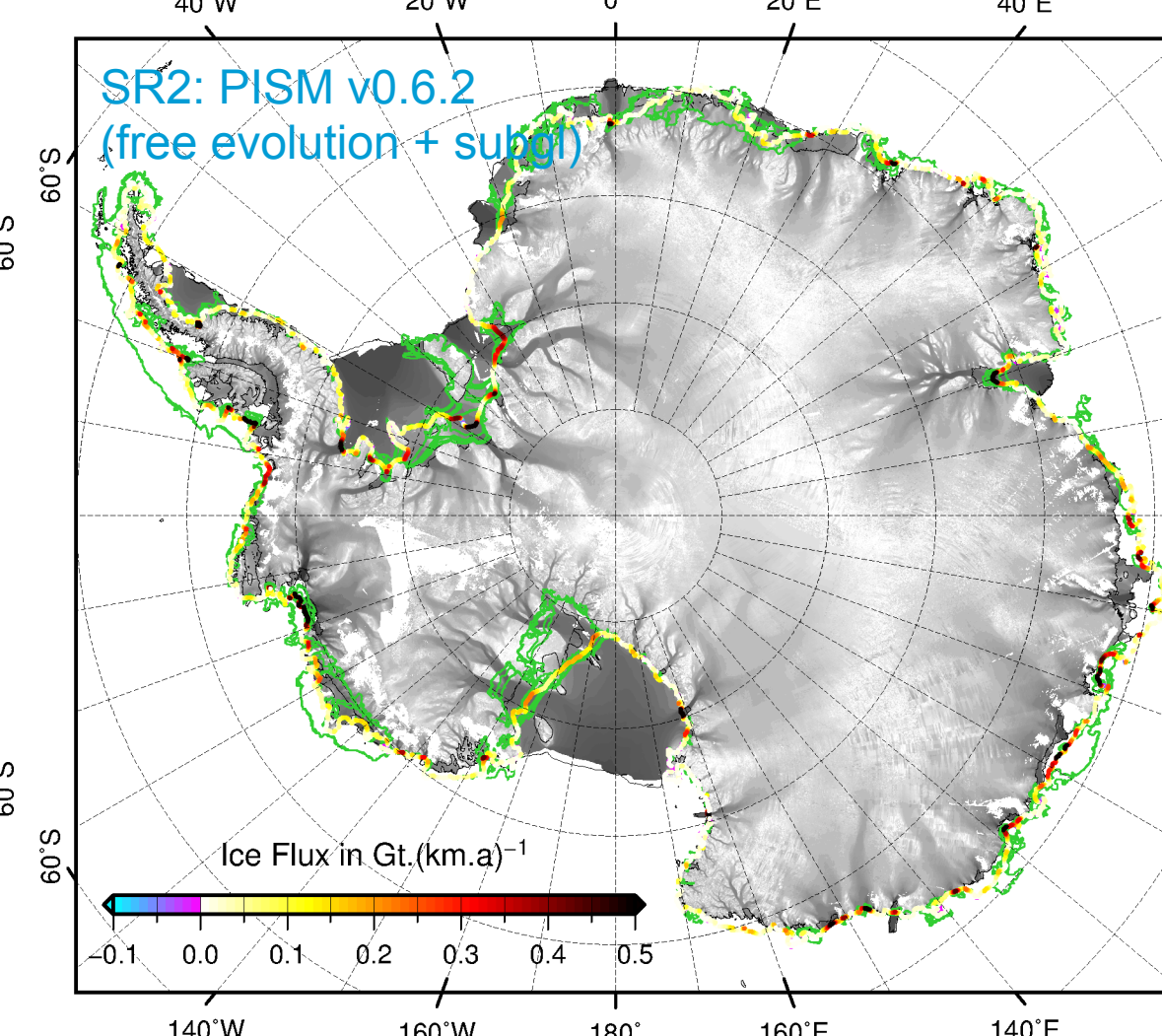
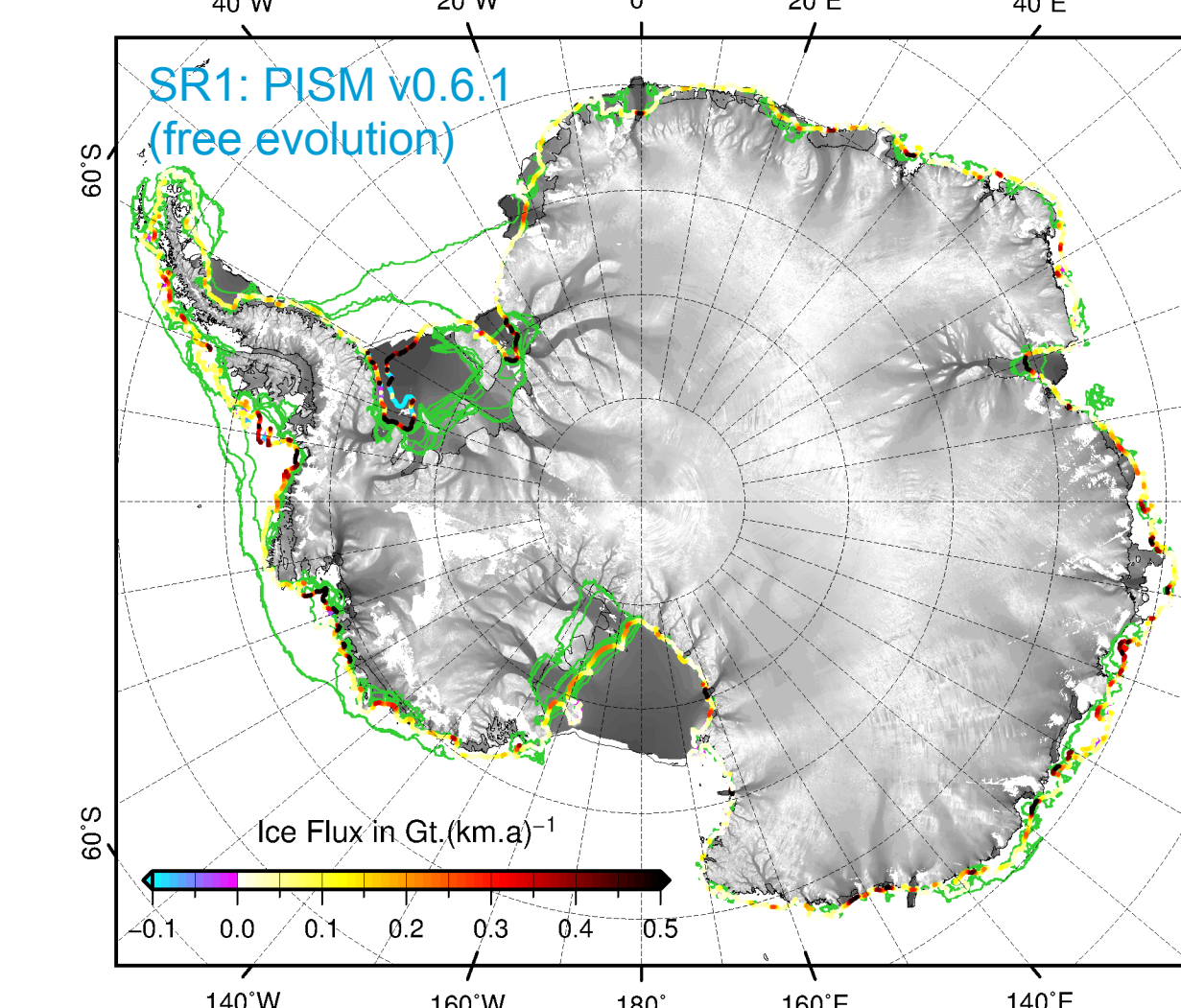


Fig. 3: Ensemble mean surface velocities for the fixed geometry simulations (FT, left) and free evolving geometry simulation (SR2, right) compared to the observed flow field (Rignot et al., 2008).

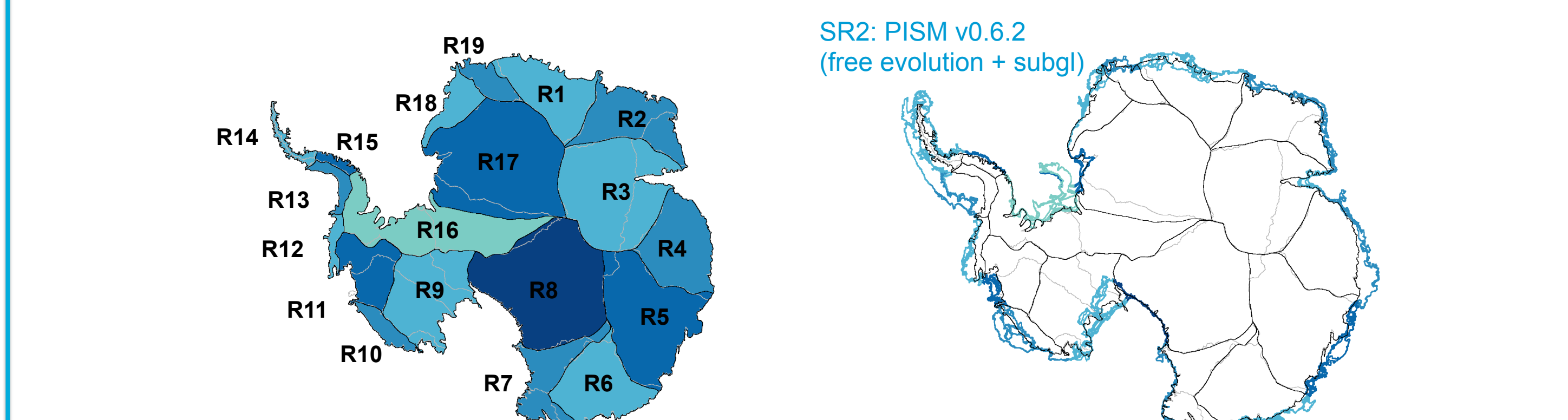


Fig. 4: Map of the drainage basins from Rignot et al., 2011 (left) and assigned drainage basins for grounding line segments after back-tracking (SR2, right). Drainage basins from Zwally et al., 2012 are shown as grey lines for comparison.

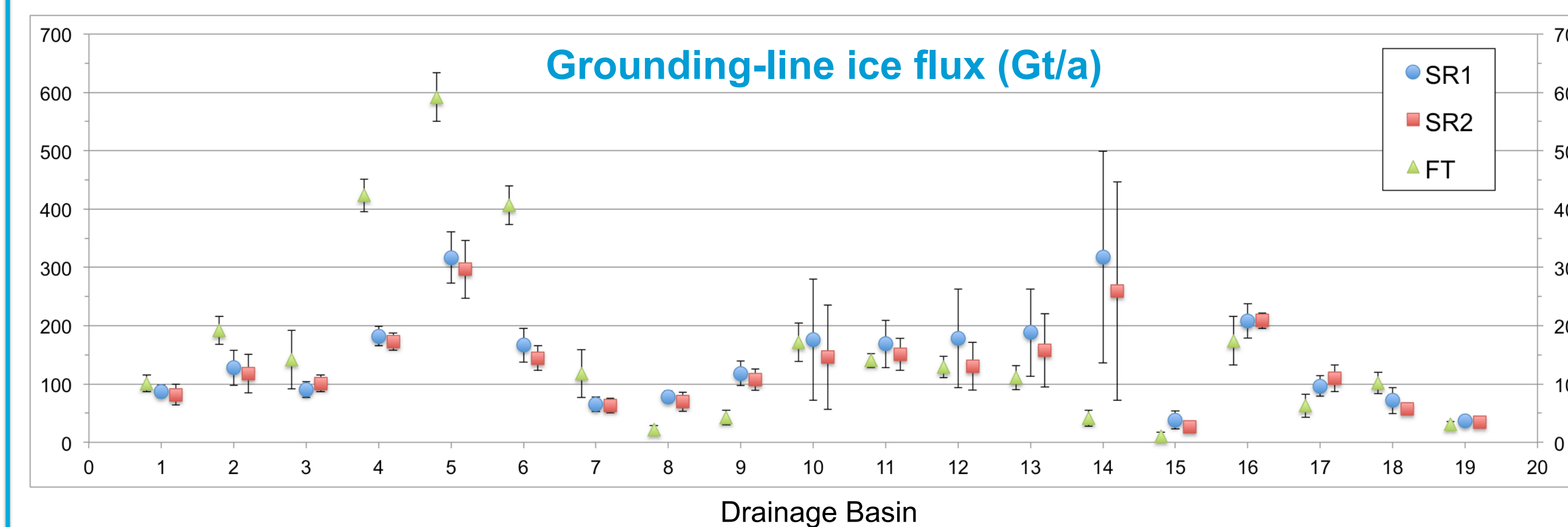


Fig. 5: Ensemble mean grounding line ice fluxes with drainage basin numbers from Rignot et al., 2011. Error bars are drawn according to the ensemble stddev within each basin.

Conclusion

- Although forced with constant climate for the entire spin-up period, a run of 4000 years for the last grid refinement step is not sufficient to reach steady state.
- The subgrid grounding line treatment improves the simulated grounding line position (most significantly in the Weddell Sea and Amundsen Sea areas).
- The simulated total ice flux over the grounding line is larger (FT: 3010±331, SR1: 2710±608, SR2: 2403±546 Gt/a) than derived from remote sensing velocities (1568±31 Gt/a, Rignot et al., 2008).
- The simulated ice flux (SR2) is larger in the three basin groups: EastAnt (60%), WestAnt (10%) and AntPen (300%) compared to Rignot et al., 2008.
- Ice flux into the large ice shelves (Filchner-Ronne: R16+R17, Amery: R3, Ross: R7+R8+R9) is relatively insensitive to different forcings (cf. R16+R17).